

Effect of local deformation on the emission energy of quantum dots in a flexible tube

Suwit Kiravittaya^{1,*}, Peter Cendula², Armando Rastelli² and Oliver G. Schmidt²

¹Max-Planck-Institut für Festkörperforschung, Heisenbergstr. 1, D-70569 Stuttgart

²Institute for Integrative Nanosciences, IFW Dresden, Helmholtzstr. 20, D-01069 Dresden

*Corresponding author: Heisenbergstr. 1, D-70569 Stuttgart, Germany, s.kiravittaya@fkf.mpg.de

Abstract: Strain induced by local deformation of a flexible micrometer-sized semiconductor tube is quantified by modeling a ball pressing on the tube wall. By changing the pressing condition, we are able to change the strain state of the tube wall incorporating self-assembled quantum dots (QDs) in the wall. The QD emission energy is calculated by solving the Schrödinger wave equation including the effects of strain induced shifts in band edges. By this technique, we demonstrate that the emission energies of two typical QDs in the flexible tube can be brought into resonance.

Keywords: Structural deformation; flexible tube; quantum mechanics; semiconductor quantum dot

1. Introduction

Wide range tuning of quantum dot (QD) emission is required for advanced studies in advanced single dot spectroscopy. Deterministic shifting of QD emission into resonance either with other QDs or optical cavity modes is highly desired. Recently, a novel technique to tune the QD emission has been proposed and experimentally demonstrated [1]. This technique is based on the local deformation of a flexible tube containing QDs in the tube wall. The large deformation produces long-range strain variations, which induce band edge energy shifts. Such variations result in a shift of the quantized energy levels of charge carriers (electrons and heavy holes) in a QD.

In this work, we model the system within MATLAB/COMSOL Multiphysics version 3.4 software environment. The strain state of a deformed tube structure is first analyzed. We quantitatively determine the tuning range of the QD emission energy produced by this local deformation. Finally, we demonstrate that this technique can be used to tune the emission energy of two QDs in the flexible tube into resonance.

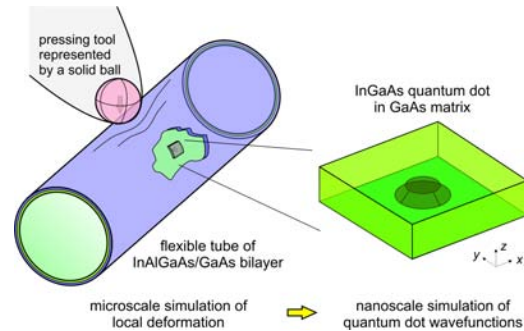


Figure 1. Schematic illustration of the flexible tube structure and a modeled QD inside the tube wall.

2. Method

2.1 Simulation of local deformation

The three-dimensional parametric analysis of solid, stress-strain in structural mechanics module is used for this study. A flexible hollow cylindrical tube, 20- μm long and with an inner diameter of 4.3- μm , is modeled. The tube wall consists of 15-nm InAlGaAs and 40-nm GaAs epitaxial layers as has been experimentally realized [1]. The long-range strain induced by local deformation (pressing) is calculated by simulating a 1- μm radius solid ball with unrealistically high Young's modulus (10^{10} GPa) moving downward to press on the outer surface of the tube wall at the center of the tube. A contact pair between the ball surface and the outer tube surface is set in order to avoid overlapping of these two domains when the pressing is simulated. Boundary surfaces at the tube openings at the front and back sides are fixed. Meshes with relatively high resolution are created in the middle of the tube in order to obtain smooth results in this part. Due to the thin wall structure, a meshing scale factor of 0.15 is used in the tube axial direction. Meshing results in ~ 20000 tetrahedral elements with 5000 mesh points (100000 degrees of freedom). The left part of figure 1 shows a schematic illustration of the

simulation process. Results from this calculation, i.e., strain components, are rotationally transformed and are further exported to the smaller domain, where an InGaAs QD is located (Right part of figure 1).

2.2 Nanoscale simulation of QD wavefunctions

In order to model a realistic system, we consider a flexible *rolled-up* GaAs/InAlGaAs microtube incorporating self-assembled QDs [1,2]. This tube is spontaneously rolling up when the strained bilayer is released from the substrate [2,3]. Due to this rolling up process, the strain gradient along the tube wall has to be taken into account. The strained InGaAs QDs inside the tube wall are modeled as truncated cones. A linear grading of indium composition (60% on top to 40% at the base) is assumed [4]. In this modeling, two QDs (40 (44) nm base diameter, 24 (28) nm top diameter, and 1.53 (1.60) nm height for QD1 (QD2)) in a $100 \times 100 \times 40$ nm³ GaAs matrix are considered. The strains originating from (i) initial rolling of the tube, which is analytically calculated [2], (ii) local deformation by pressing (imported from the former calculation), and (iii) partial relaxation of strains in the QD material [5] (which is calculated prior to the wavefunction calculation), are superimposed. Then, shifts of conduction band and valence band edges are calculated using deformation potential theory [6]. The three-dimensional Schrödinger's equation with single band effective mass approximation is solved for electron and heavy-hole quantized energies and their wavefunctions. Eigenvalue analysis in PDE, coefficient form is used. The material parameters used in the calculation are listed in Table I. Linear interpolation between GaAs and InAs is used for In_xGa_{1-x}As material with the exception of the In_xGa_{1-x}As bandgap E_g . A band offset ($\Delta E_c/\Delta E_g$) of 0.83 is assumed. The QD transition (emission) energy is defined by the difference in energy level of electron and heavy hole (no Coulomb interaction is included).

Table I. Material parameters used in the wavefunction calculations [5,6]

	GaAs	InAs
a_0 (nm)	0.56533	0.60584
C_{11} (GPa)	118.79	83.29
C_{12} (GPa)	53.76	45.26
C_{44} (GPa)	59.4	39.6
E_g (eV)	$1.5194 - 1.6114x + 0.51x^2$	
a (eV)	-8.33	-6.08
a_c (eV)	-7.17	-5.08
b (eV)	-1.70	-1.80
d (eV)	-4.55	-3.6
m_e (m_0)	0.067	0.023
$m_{hh,xy}$ (m_0)	0.120	0.035
$m_{hh,z}$ (m_0)	0.341	0.500
m_0 = free electron mass ($9.11 \cdot 10^{-31}$ kg)		

3. Numerical Results

3.1 Tube deformation

Figure 2 shows the total displacement induced by the local deformation. In this calculation, the pressing force is directed towards the center of the tube. The solid ball is displaced along the tube radius by a distance in the range 0-1000 nm, which is a predefined parametric constraint. Using a force constraint within a few hundreds μ N range is a possible alternative. However, we find that the results by both constraints are quantitatively similar. Due to the stress interaction between the ball and the tube, there are both compressive and tensile parts on the tube wall. Increasing the tube length to more than 20 μ m changes the results only negligibly.

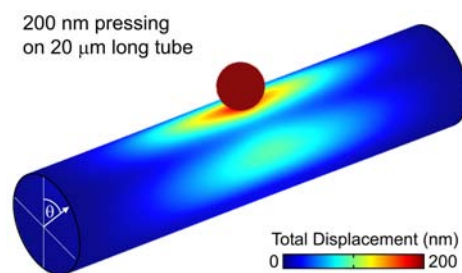


Figure 2. Calculated deformed shape of a flexible 20- μ m long tube after pressing with a 1- μ m radius ball at its center. The ball is displaced by 200 nm along the tube radius.

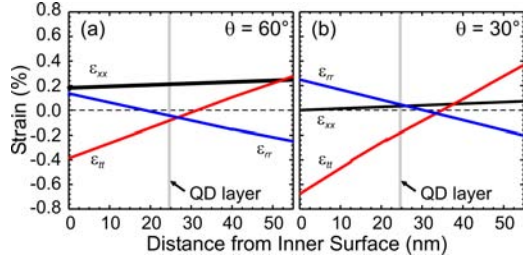


Figure 3. Normal strain components originating from the local deformation as a function of distance from the inner surface at (a) $\theta = 60^\circ$ and (b) $\theta = 30^\circ$. QDs in the QD layer at $\theta = 60^\circ$ (30°) have an additional tensile (compressive) strain due to the pressing.

As an example, figure 3 shows two plots of the strain components at the azimuthal angle θ of 60° and 30° (see figure 2) in the *pressing plane* (the plane perpendicular to the tube axis at the center of the tube). In figure 3(a), the volumetric strain ε_{vol} , which is defined as $\varepsilon_{rr} + \varepsilon_{tt} + \varepsilon_{xx}$, where ε_{rr} , ε_{tt} , and ε_{xx} are normal strain components in tube radial, tangential and axial directions, respectively, is mainly positive indicating the tube wall is in a tensile strain state. The gradients of the normal strain components along the tube wall are clearly observed while the amplitudes of all shear strain components are typically negligible ($< 0.05\%$ under this condition, not shown). If we consider only the position of the modeled QD layer (25 nm from the inner tube surface), a QD at θ of 60° (figure 3(a)) experiences additional tensile strain while a QD at 30° (figure 3(b)) has additional compressive strain. Since linear elasticity is used, the magnitudes of each strain component are proportional to the applied pressing force and ball displacement.

3.2 QD wavefunctions and transition energy

Figures 4(a) and 4(b) show isosurfaces of the square of ground state electron ($|\psi_e|^2$) and heavy hole ($|\psi_{hh}|^2$) wavefunctions of carriers confined in QD1, which is assumed to be located at $\theta = 60^\circ$ in the pressing plane when there is no effects of strain from the pressing. $|\psi_e|^2$ and $|\psi_{hh}|^2$ look similar in the perspective view and have flat circular shape, since circular symmetry shape is assumed for this QD. These wavefunctions are mainly confined in the top part of the dot due to the lower bandgap (high indium content) in that

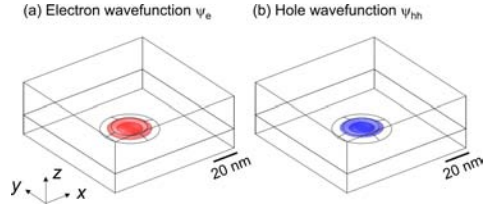


Figure 4. Typical square of wavefunctions of (a) electron and (b) heavy hole confined in the InGaAs QD in GaAs matrix inside the tube wall. The isosurfaces of $0.1 \cdot |\psi|^2$ and $0.9 \cdot |\psi|^2$ are shown. Due to the large lateral QD size and small height (diameter 40 nm, 1.53 nm height), the wavefunctions are rather flat.

region. When the pressing is applied there is a slight change of their shapes (shown below) depending on the applied pressing force. Note that the wavefunctions of the excited states are also obtained from the calculation. However, since we are interested in the ground state transition energy (main optical emission peak from the recombination of electron and hole in a single QD), the other excited state wavefunctions are not considered here.

The band edge profiles as well as the magnitude of the carrier wavefunctions (in arbitrary units) along the center of QD1 (z -axis in this small domain calculation) are plotted in figure 5. The quantized ground state energy levels of both electron and heavy hole are shown at two pressing levels (without pressing and with 1000-nm ball displacement). The initial band edge without pressing is slightly tilted due to the strain induced by the rolling up process [2]. The bandgap inside the QD is initially smaller on the top part due to the high indium content (60%) in this part. As expected from deformation potential theory [6], the additional tensile strain due to pressing (for a QD at $\theta = 60^\circ$ cf. figure 3(a)) induces a bandgap lowering of both the InGaAs QD and the GaAs matrix. This results in a lowering of the QD transition energy. For the conduction band edge, the overall strain homogeneously shifts the band edge inside the QDs while the heavy hole level is influenced by both volumetric compressive strain and shear strain, which counter-shift this band edge. Due to the change of the band edge potential, the electron wavefunction is slightly modified due to the pressing while the heavy-hole wavefunction is practically unchanged. With a 1000-nm deformation, a pronounced lowering of the electron quantized energy is obtained.

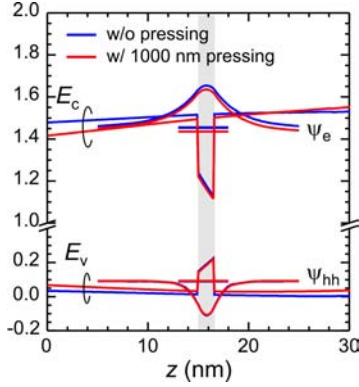


Figure 5. Calculated band edge profile of conduction band (E_c) and valence band (E_v), electron (ψ_e) and hole (ψ_{hh}) wavefunctions along z -direction through the center of a QD located at $\theta = 60^\circ$ (QD1). The corresponding quantized energy levels of electron and heavy hole are shown. Blue and red lines are results when the strain induced by local deformation is excluded and included, respectively.

4. Demonstration of Resonant QDs

Based on the study of pressing effects on the QD transition energy discussed in the former section, we propose this method as a technique to tune QD emissions after their fabrication. Since in general the emission energy of a self-assembled QD is determined by its size, shape, and composition, which can hardly be individually modified after the fabrication step, it is highly desired to have a technique to locally and reversibly tune its emission [7]. Here, we consider QD1 and QD2 having the size and shape described in section 2.2. QD1 (QD2) is located in the QD layer (see figure 3) at an azimuthal position θ of 60° (30°) relative to the pressing point ($\theta=0^\circ$). Both QDs are in the pressing plane. By pressing with suitable pressing magnitude, we are able to tune both QD emission into resonance.

Figure 6 shows the QD transition energies as a function of pressing magnitude for QD1 and QD2. Due to the fact that QD2 is slightly larger than QD1, the initial QD transition energy of QD2 is lower than that of QD1 (1.351 eV vs. 1.364 eV). Pressing induces a lowering of QD

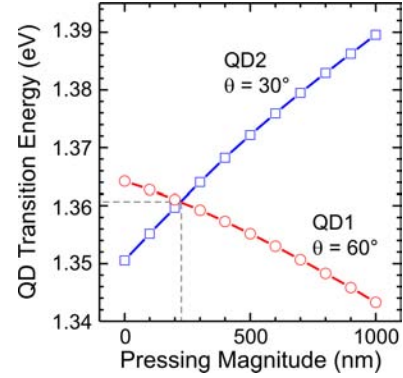


Figure 6. Calculated QD transition energy as a function of pressing magnitude. The QD1 at $\theta = 60^\circ$ shows a redshift of the emission while a blueshift is observed for QD2 located at $\theta = 30^\circ$. Resonant energies of these two QDs (1.3607 eV) are observed at a pressing magnitude of ~ 220 nm.

transition energy of QD1 due to the additional tensile strain while at the same time it induces compressive strain in QD2. The QD1 is redshifted by 21 meV/nm while QD2 is blueshifted by 39 meV/nm. The resonant state of these two QDs at 1.3607 eV is obtained when a pressing magnitude of ~ 220 nm is applied. Resonant emission can be achieved for a wide range of different QD sizes, shapes, compositions, and locations.

5. Conclusions

We have presented a numerical study of the shifts of QD emission energies due to a local deformation obtained by pressing a flexible microtube structure. The induced strain, changes of carrier wavefunctions and their quantized energies were quantitatively determined. Finally, we have demonstrated that by tuning the pressing magnitude emissions from two QDs in the tube can be brought into resonance. This work provides a deep insight into a novel tuning technique of QD emission energy, which is required for future manipulation in advanced single QD spectroscopy. Based on this work, simulations of pressing and deforming of other flexible structures (microrings, nanomembranes, cantilevers, etc.) are also possible.

6. References

1. S. Mendach, S. Kiravittaya, A. Rastelli, M. Benyoucef, R. Songmuang, and O. G. Schmidt, Bidirectional wavelength tuning of individual semiconductor quantum dots in a flexible rolled-up microtube, *Phys. Rev. B*, **78**, 035317 (2008).
2. S. Mendach, R. Songmuang, S. Kiravittaya, A. Rastelli, M. Benyoucef, and O. G. Schmidt, Light emission and wave guiding of quantum dots in a tube, *Appl. Phys. Lett.*, **88**, 111120 (2006).
3. O. G. Schmidt and K. Eberl, Thin solid films roll up into nanotubes, *Nature (London)*, **410**, 168 (2001)
4. D. M. Bruls *et al.*, Determination of the shape and indium distribution of low-growth-rate InAs quantum dots by cross-sectional scanning tunneling microscopy, *Appl. Phys. Lett.*, **81**, 1708 (2002)
5. M. Grundmann, O. Stier, and D. Bimberg, InAs/GaAs pyramidal quantum dots: Strain distribution, optical phonons, and electronic structure, *Phys. Rev. B*, **52**, 11969 (1995).
6. C. G. Van der Walle, Band lineups and deformation potentials in the model-solid theory, *Phys. Rev. B*, **39**, 1871 (1989).
7. A. Rastelli, A. Ulhaq, S. Kiravittaya, L. Wang, A. Zrenner, and O. G. Schmidt, *In situ* laser microprocessing of single self-assembled quantum dots and optical microcavities, *Appl. Phys. Lett.*, **90**, 073120 (2007).

7. Acknowledgements

We acknowledge Dr. Stefan Mendach for motivating this topic and Dr. Vlastimil Krapek for a fruitful discussion. This work was financially supported by BMBF (Contract No. 03N8711) and the DFG (Contracts No. Schm1298/5-1, AR1634/1-1).